

# Motion-free hybrid design laser beam propagation analyzer using a digital micromirror device and a variable focus liquid lens

Mumtaz Sheikh and Nabeel A. Riza\*

Photonic Information Processing Systems Laboratory, CREOL, The College of Optics and Photonics, University of Central Florida, 4000 Central Florida Boulevard, Orlando, Florida 32816-2700, USA

\*Corresponding author: riza@creol.ucf.edu

Received 25 August 2009; accepted 3 October 2009;  
posted 30 November 2009 (Doc. ID 115781); published 7 January 2010

To the best of our knowledge, we propose the first motion-free laser beam propagation analyzer with a hybrid design using a digital micromirror device (DMD) and a liquid electronically controlled variable focus lens (ECVFL). Unlike prior analyzers that require profiling the beam at multiple locations along the light propagation axis, the proposed analyzer profiles the beam at the same plane for multiple values of the ECVFL focal length, thus eliminating beam profiler assembly motion. In addition to measuring standard Gaussian beam parameters, the analyzer can also be used to measure the  $M^2$  beam propagation parameter of a multimode beam. Proof-of-concept beam parameter measurements with the proposed analyzer are successfully conducted for a 633 nm laser beam. Given the all-digital nature of the DMD-based profiling and all-analog motion-free nature of the ECVFL beam focus control, the proposed analyzer versus prior art promises better repeatability, speed, and reliability. © 2010 Optical Society of America

OCIS codes: 140.3295, 120.4800, 350.5500.

## 1. Introduction

A Gaussian laser beam is completely characterized for all distances from the source by only two parameters, i.e., the minimum beam waist radius  $w_0$  and the location of the minimum waist  $z_0$  [1]. Precise knowledge of these values is critical for many applications including, but not limited to, laser manufacturing, machining, optical communications, materials research, optical metrology, radar, and laser damage studies. In principle,  $w_0$  can be determined by a single beam radius measurement at a large distance from the source [2] or in the focal plane of a fixed lens placed in the beam path [3,4]. In addition, the interference pattern in an unfocused beam generated using a birefringent crystal gives a measure of  $w_0$  [5]. However, to determine  $z_0$  one must measure the beam radius at multiple locations along the beam

path [2,6,7]. This multiple measurement process requires either the motion of optical elements in the beam path or the motion of the entire beam profiler assembly over large distances, e.g., twice the Rayleigh range [8], leading to a beam analyzer that is slow, cumbersome, and inherently suffers from poor measurement repeatability. Beam profilers used to measure the beam radii are dominated by mechanical knife-edge scanning techniques [2,9,10]. Other less commonly used mechanical techniques include sliding slit [11], translating pinhole [12], rotating mirror [13], surface plasmon polaritons [14], and encircled energy principal-based profilers [15]. These mechanical techniques have limited repeatability as they require high-resolution precision motion systems that are not only expensive but deploy continuous transverse-direction analog translation of components. A new class of all-digital and hybrid analog-digital spatial light modulator (SLM)-based profilers has been introduced that use a digital micromirror device (DMD) [16–20] and liquid crystal

---

0003-6935/10/1600D6-06\$15.00/0  
© 2010 Optical Society of America

display (LCD) [21] technologies. The all-digital version of these beam profilers offers the benefit of excellent SLM chip-based reliability and 100% repeatability in beam profiling by digital-mode chip operations over instrument lifetimes.

In Section 2 we introduce and demonstrate a new motion-free beam analyzer instrument that engages an electronically controlled variable focus lens (ECVFL) in conjunction with an all-digital DMD-based beam profiler to accurately measure the parameters of a Gaussian laser beam, i.e.,  $w_0$  and  $z_0$ . Such an analyzer design does not require any motion of optical elements or a beam profiler assembly, thus eliminating a key limitation of prior art analyzers. In Section 3 we describe the proposed beam propagation analyzer optical design and its experimental results. In Section 4 we show how the proposed analyzer can be used to measure the  $M^2$  beam propagation parameter [22,23] of a laser beam. Our conclusions are given in Section 5.

## 2. Proposed Motion-Free Beam Propagation Analyzer

Figure 1 shows the proposed beam propagation analyzer system. The Gaussian laser beam to be analyzed passes through the ECVFL with a tunable focal length  $f$  and strikes the DMD placed a fixed distance  $d_2$  from the electronically controlled lens. A Gaussian beam optical field at a radial distance  $r$  from the optic axis and at a distance  $z$  along the beam travel or optic-axis direction can be represented in terms of its complex  $q$  parameter as [1]

$$\psi(r, z) \propto \exp\left(\frac{-jkr^2}{2q(z)}\right), \quad (1)$$

where

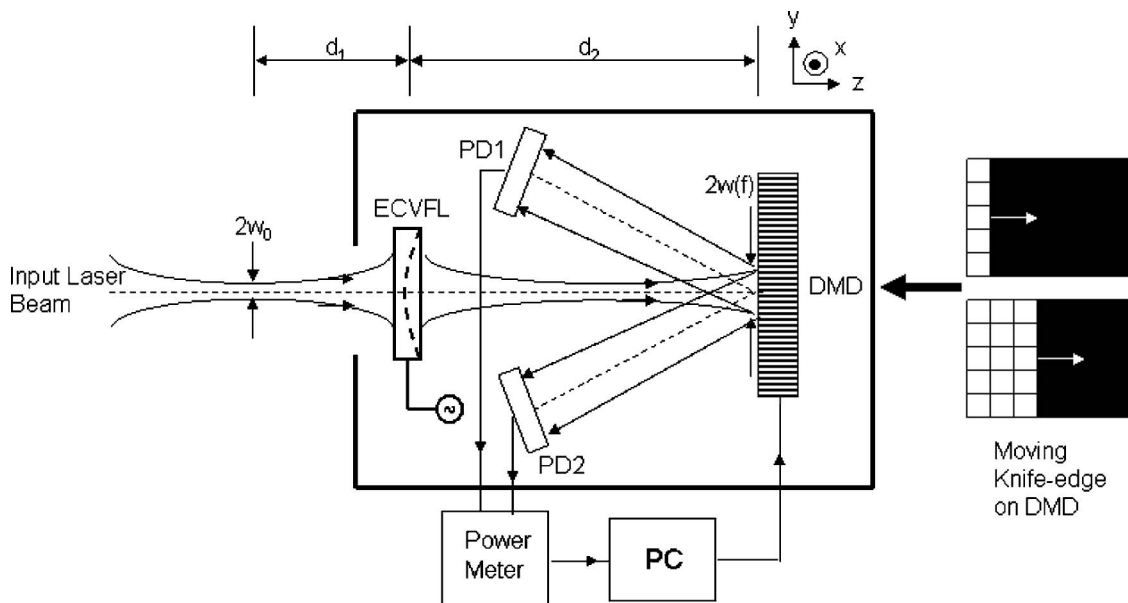


Fig. 1. Proposed motion-free hybrid-design laser beam propagation analyzer system using a DMD and an ECVFL: PD1/PD2, photodetectors; PC, personal computer.

$$\frac{1}{q(z)} = \frac{1}{R(z)} - j\frac{\lambda}{\pi w^2(z)}. \quad (2)$$

Here  $w(z)$  is the  $1/e^2$  beam radius,  $R(z)$  is the beam radius of curvature,  $\lambda$  is the laser wavelength, and  $k = 2\pi/\lambda$ . At the minimum beam waist location  $z_0$ , a distance  $d_1$  in front of the ECVFL, the phase front is plane with  $R(z) = \infty$ . Using Eq. (2), the  $q$  parameter  $q_0$  at the minimum beam waist location can be written in terms of the minimum beam radius  $w_0$  as

$$\frac{1}{q_0} = -j\frac{\lambda}{\pi w_0^2} \equiv \frac{1}{jz_R}, \quad (3)$$

where  $z_R$  is known as the Rayleigh range. After passing through the ECVFL, the laser beam  $q$  parameter  $q_1$  at the DMD plane is given by [1]

$$q_1 = \frac{Aq_0 + B}{Cq_0 + D} = \frac{Ajz_R + B}{Cjz_R + D}. \quad (4)$$

Here,  $A$ ,  $B$ ,  $C$ , and  $D$  are the elements of the  $ABCD$  matrix that defines the transfer of paraxial rays through the optical system defined between the ECVFL and the DMD. The  $ABCD$  matrix for this complete system is a product of three  $ABCD$  matrices, specifically, one for  $d_1$  distance free-space propagation, one for transmission through a thin lens with focal length  $f$ , and one for distance  $d_2$  free-space propagation. Hence, the required  $ABCD$  matrix is given by

$$\begin{aligned} \begin{bmatrix} A & B \\ C & D \end{bmatrix} &= \begin{bmatrix} 1 & d_2 \\ 0 & 1 \end{bmatrix} \begin{bmatrix} 1 & 0 \\ -1/f & 1 \end{bmatrix} \begin{bmatrix} 1 & d_1 \\ 0 & 1 \end{bmatrix} \\ &= \begin{bmatrix} 1 - d_2/f & d_1 + d_2 - d_1 d_2/f \\ -1/f & 1 - d_1/f \end{bmatrix}. \end{aligned} \quad (5)$$

Equation (4) can be rewritten as

$$\frac{1}{q_1} = \frac{Cjz_R + D}{Ajz_R + B} = \frac{(Cjz_R + D)(-Ajz_R + B)}{A^2z_R^2 + B^2}. \quad (6)$$

Separating the real and imaginary parts, one can rewrite Eq. (6) as

$$\frac{1}{q_1} = \frac{ACz_R^2 + BD}{A^2z_R^2 + B^2} - j \frac{z_R(AD - BC)}{A^2z_R^2 + B^2}. \quad (7)$$

Comparing Eq. (7) with Eq. (2), one can write

$$\text{Im} \left\{ \frac{1}{q_1} \right\} = -\frac{\lambda}{\pi w^2(f)} = -\frac{z_R(AD - BC)}{A^2z_R^2 + B^2}, \quad (8)$$

where  $w(f)$  is the  $f$ -dependent  $1/e^2$  beam radius on the DMD plane. Substituting the values of  $A$ ,  $B$ ,  $C$ , and  $D$  from Eq. (5) and the value of  $z_R$  from Eqs. (3) and (8) can be simplified to

$$w^2(f) = w_0^2(1 - d_2/f)^2 + \frac{\lambda^2}{\pi^2 w_0^2} (d_1 + d_2 - d_1 d_2/f)^2, \quad (9)$$

Next, Eq. (9) can be rewritten as

$$w^2(f) = w_0^2 \left[ (1 - d_2/f)^2 + \left\{ \frac{\lambda(d_1 + d_2 - d_1 d_2/f)}{\pi w_0^2} \right\}^2 \right]. \quad (10)$$

In Eq. (10),  $d_2$  is known and is fixed, whereas  $d_1$  and  $w_0$  are unknown laser beam parameters. By varying  $f$  and measuring the corresponding value of  $w(f)$ , a set of simultaneous equations in  $d_1$  and  $w_0$  can be found. Since there are two unknowns, a minimum of two readings is required although more readings should be taken so that  $d_1$  and  $w_0$  are determined in the least-squares sense to account for experimental errors. Note that, if the actual minimum beam waist location is behind the ECVFL (and not in front of the ECVFL as shown in Fig. 1), then  $d_1$  would result as a negative value. Once  $w_0$  is determined from the calculations, the beam divergence half-apex angle can be found using [1]

$$\theta = \frac{\lambda}{\pi w_0}. \quad (11)$$

To measure  $w(f)$ , knife-edge beam profiling using the DMD-based beam profiler is employed [16,17]. Using software control, each micromirror on the

DMD can be individually set to either a  $+\theta$  or a  $-\theta$  tilt state. A virtual knife-edge is formed on the DMD by setting some micromirrors to  $+\theta$  (black pixels in Fig. 1) and the rest to the  $-\theta$  tilt position (clear pixels in Fig. 1). Photodetectors PD1 and PD2 are set symmetrically along the optic axis such that light reflecting off the mirrors in the  $+\theta$  state falls on PD1; light reflecting off the mirrors in the  $-\theta$  state falls on PD2. This virtual knife-edge slides across the incident beam, and the PD1 and PD2 power is simultaneously recorded. The use of two photodetectors is important for normalization of the detected power when the laser beam power fluctuates during profiling operations [18]. Next an error function is fit to the acquired data and from this error-function fit,  $1/e^2$  beam radius  $w(f)$  is determined [10]. The resolution of this measurement is equivalent to the pixel pitch of the DMD.

### 3. Experimental Demonstration

The Fig. 1 analyzer is set up as a proof-of-concept experiment in the laboratory. A 10 mW  $\lambda = 632.8$  nm Melles Griot (Albuquerque, New Mexico) Model 05-LHP-991 He-Ne laser source is used as the input laser beam. The ECVFL used is a Varioptic (Lyon, France) Arctic 320 liquid lens with a 3 mm clear aperture. The liquid lens is a broadband adjustable multifocus imaging lens that changes focus due to the electrowetting process [24]. The calibration curve for the liquid lens focal length versus the AC drive signal is specified in the product data sheet [24]. The response of the liquid lens is highly repeatable for a liquid lens focal length  $f > 7.7$  cm [25]. The visible band Texas Instruments (TI) (Dallas, Texas) DMD used has an extended graphics array (XGA) format of  $1024 \times 768$  micromirrors with a pixel pitch of  $13.68 \mu\text{m}$ , and  $\theta = 12^\circ$ , and is placed a fixed distance  $d_2 = 30.8$  cm from the ECVFL. The profiler detectors PD1 and PD2 are Newport (Irvine, California) Model 918D-UV having a spectral range of 200–1100 nm and an active area of  $1 \text{cm}^2$ . The powermeter is a dual-channel Newport Model 2931C with a nanowatt optical power measurement resolution.

Focal length  $f$  of the ECVFL is tuned by varying the AC drive signal duty cycle. For each value of  $f$ , the beam is profiled using the DMD-based profiler. For a value of  $f = 9.6$  cm, Figs. 2(a) and 2(b) show the normalized raw optical power data acquired for the DMD programmed moving knife-edges across the beam horizontal and vertical directions, respectively. The raw data are fit with an error function [Figs. 2(c) and 2(d)] to generate Gaussian profiles for the DMD plane laser beam. According to the fit, the horizontal  $1/e^2$  beam radius  $w_H(f = 9.6 \text{ cm})$  is found to be  $734.05 \mu\text{m}$ ; the vertical  $1/e^2$  beam radius  $w_V(f = 9.6 \text{ cm})$  is found to be  $729.83 \mu\text{m}$ . By multiplying the 1-D horizontal and vertical Gaussian profiles found using the error-function fits, Figs. 2(e) and 2(f) show the gradient and spatial views of the generated 2-D beam profile, respectively. In a similar manner, the beam is profiled using the DMD-based profiler for

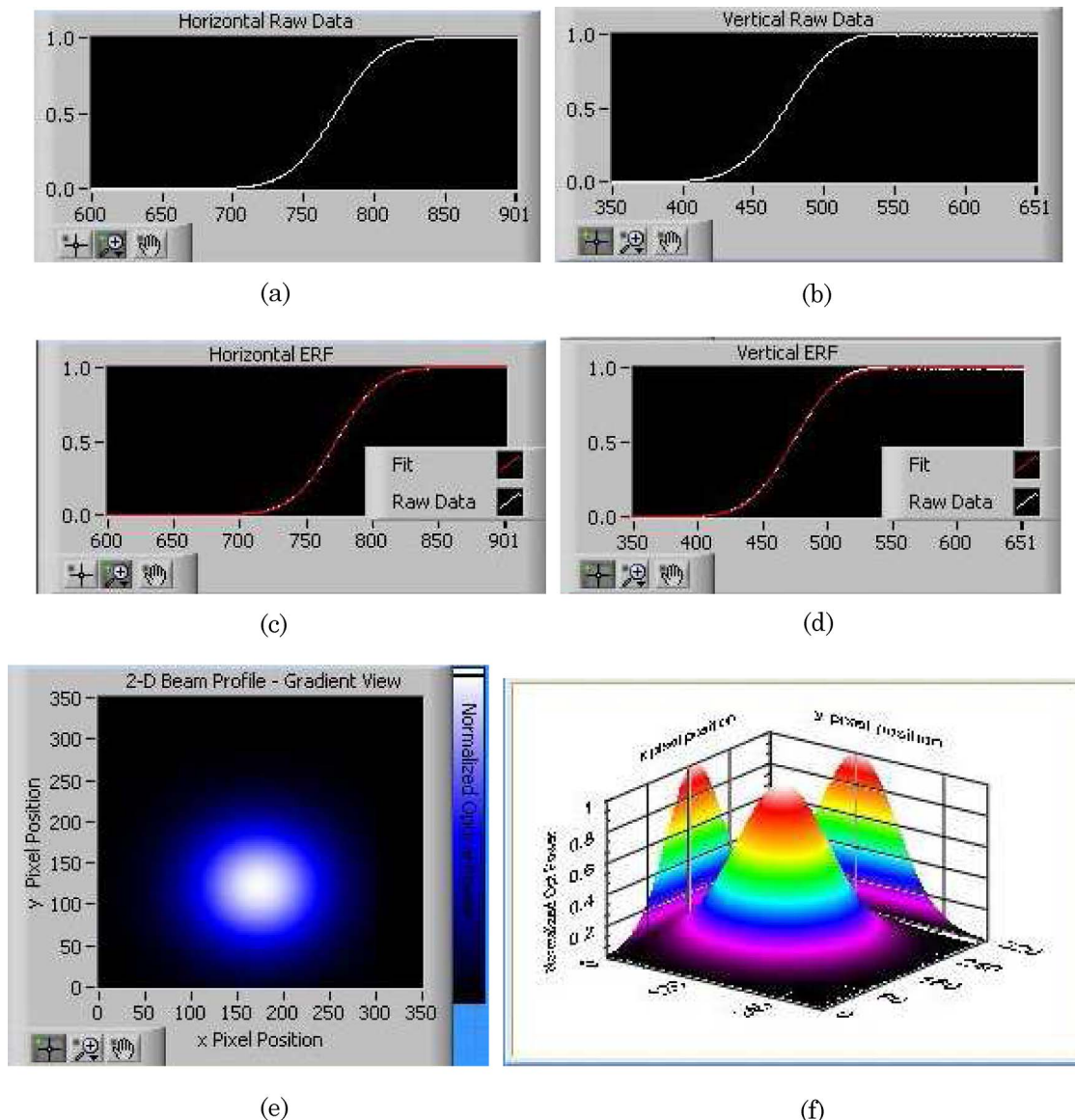


Fig. 2. (Color online) For the 633 nm laser beam, DMD knife-edge beam profiling results for the  $f = 9.6$  cm ECVFL. Knife-edge raw optical power data along the test beam (a) horizontal direction and (b) vertical direction. Error-function fit for (c) horizontal knife-edge data and (d) vertical knife-edge data. Two-dimensional beam profile (e) gradient view and (f) spatial view.

other values of  $f$ . Table 1 shows the measured horizontal and vertical  $1/e^2$  beam radii  $w_H(f)$  and  $w_V(f)$  corresponding to each value of  $f$ . Note that the values of  $f$  are selected such that the ECVFL is essentially aberration free, typically with the ECVFL  $f$  number greater than 20, implying weak lens operations [8]. For example, for a 3 mm diameter ECVFL,  $f > 6$  cm. In addition, the value of  $d_2$  is set of the order of  $f$ , because a longer  $d_2$  would result in the laser beam expanding more than the size of the DMD and a shorter  $d_2$  would result in not enough change in the values of beam radii when  $f$  is varied to give an accurate curve fit.

Table 1 data are curve fits to Eq. (10) with known fixed parameters of  $\lambda = 632.8$  nm and  $d_2 = 30.8$  cm using the Levenberg–Marquardt algorithm [26]. Note that, given that the ECVFL diameter is 3 mm,

the weak lensing condition is satisfied as the  $f$  used are greater than 6 cm. Figures 3(a) and 3(b) show the curve-fitting results for the horizontal and the vertical beam radii, respectively. The curve fit gives the values of the unknown parameters  $w_{0H} = 324.27$   $\mu\text{m}$ ,  $d_{1H} = 25.8$  cm,  $w_{0V} = 324.71$ , and  $d_{1V} = 25.1$  cm.

Table 1. Corresponding Values of the ECVFL <sup>a</sup>

$f$ (cm)	$w_H(f)$ ( $\mu\text{m}$ )	$w_V(f)$ ( $\mu\text{m}$ )
9.6	734.05	729.83
11.5	549.99	550.78
13.6	412.82	415.72
22.9	177.77	173.87
33.0	208.41	206.07

<sup>a</sup>Focal length  $f$  and the measured  $1/e^2$  laser beam horizontal  $w_H(f)$  ( $\mu\text{m}$ ) and vertical  $w_V(f)$  ( $\mu\text{m}$ ) radii.

Next, using Eq. (11) the beam divergence half-apex angle for both the horizontal and the vertical directions is found to be  $\theta = 0.62$  mrad. These analyzer measured values compare well with the Melles Griot laser data sheet values of a minimum beam radius of  $w_0 = 325 \mu\text{m}$  and a beam divergence half-apex angle of  $\theta = 0.62$  mrad. Note that, theoretically, the accuracy of the beam waist measurement is limited by the DMD pixel pitch, although in practice the accuracy is expected to be better because of using more than two pairs of  $f$  and  $w(f)$  values and the use of least-squares curve fitting would, in general, even out the errors. The physical distance between the ECVFL and the laser aperture in the experiment is 22.9 cm. Given the average analyzer measured  $d_1$  value is  $(25.1 + 25.8)/2 = 25.45$  cm, the minimum beam waist is estimated to be formed as  $25.45 - 22.9 = 2.55$  cm inside the laser.

#### 4. Measurement of Beam Propagation Parameter $M^2$

The beam propagation parameter  $M^2$  is a measure of the quality of the laser beam, i.e., how close a given laser beam is to an ideal fundamental  $\text{TEM}_0$  Gaussian mode and is given by the square of the ratio of the laser beam divergence to the beam divergence of an ideal Gaussian beam with the same minimum beam waist [22,23]. Since Eq. (10) fits the data points from the conducted experiment extremely well (see Fig. 3), it can be concluded that this particular laser beam is close to a pure Gaussian, i.e., the fundamental mode  $\text{TEM}_0$  is dominant, implying a value of  $M^2$  close to 1. However, the same technique can be used to estimate laser beam parameters for multimode laser beams by incorporating the  $M^2$  factor into Eq. (10). For multimode beams, the beam radius is  $M$  times larger everywhere in comparison with the embedded fundamental mode [22]. Therefore, the multimode beam radius  $W(f)$  at the DMD plane and the minimum beam radius  $W_0$  can be written in terms of the corresponding fundamental mode radii as [22]

$$W_0 = Mw_0, \quad W(f) = Mw(f). \quad (12)$$

Inserting Eq. (12) into Eq. (10) yields

$$W^2(f) = W_0^2 \left[ (1 - d_2/f)^2 + \left\{ \frac{M^2 \lambda (d_1 + d_2 - d_1 d_2/f)}{\pi W_0^2} \right\}^2 \right]. \quad (13)$$

In this case, in addition to  $W_0$  and  $d_1$ , there is a third unknown parameter  $M$ . Therefore at least three sets of  $f$  and  $W(f)$  readings are required to find the unknown parameters. Unlike fundamental-mode Gaussian beams where the  $1/e^2$  beam radius definition is used, for multimode beams the International Standards Organization (ISO) has recommended a second-moment radius definition to be used as the standard for a beam radius [27]. According to this

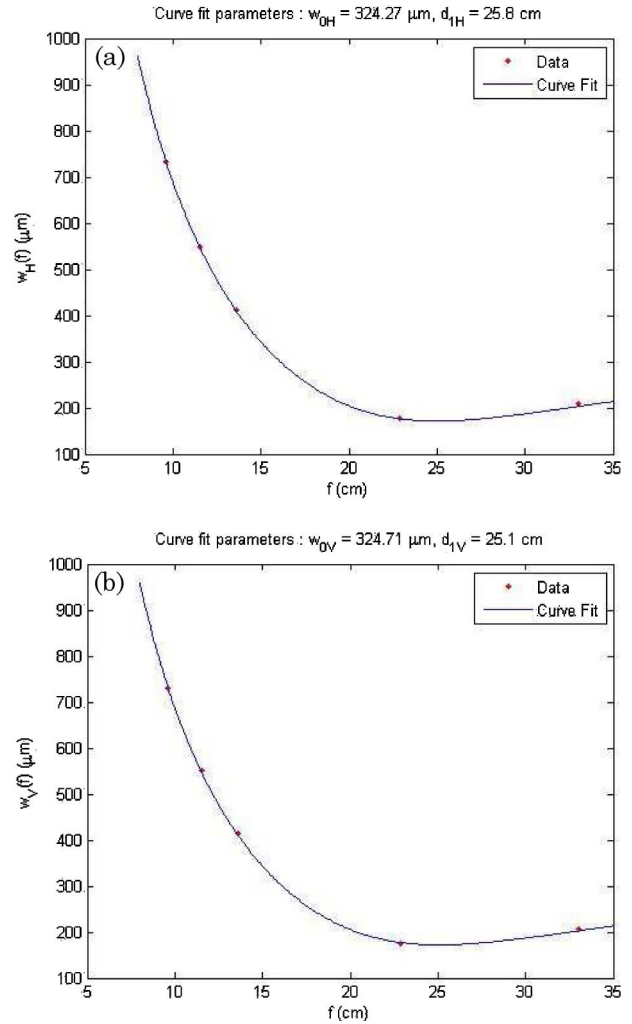


Fig. 3. (Color online) Table 1 data and Eq. (10) provided the least-squares curve fit for determining the test 633 nm laser beam (a) horizontal beam radius  $w_H(f)$  and (b) vertical beam radius  $w_V(f)$ .

definition, the beam radius is given by twice the standard deviation of the irradiance distribution of the laser beam as sampled by a pinhole translated across the beam [23]. Most importantly, the second-moment beam radius  $W(f)$  can also be readily measured using the DMD-based profiler as a pinhole profiler [20]. In this case, a virtual pinhole is moved across the DMD and the corresponding PD1 and PD2 power data are recorded to generate a pinhole irradiance profile  $I(x,y)$  of the incident laser beam. The second-moment horizontal beam radius  $W_H(f)$  is then given by [23]

$$W_H(f) = 2 \sqrt{\frac{\sum_x \sum_y I(x,y) (x - x_0)^2}{\sum_x \sum_y I(x,y)}}, \quad (14)$$

where

$$x_0 = \frac{\sum_x \sum_y I(x,y) x}{\sum_x \sum_y I(x,y)}. \quad (15)$$

$x_0$  is the centroid of the beam in the  $x$  direction. In the same way, the vertical direction beam radius  $W_V(f)$  can be calculated. Once  $W_0$  and  $M$  are determined by least-squares curve fitting, the multimode laser beam divergence is calculated as [22]

$$\Theta = \frac{M^2 \lambda}{\pi W_0}. \quad (16)$$

Note that the prior art techniques [8,28,29] rely on measuring second-moment beam radii using mechanically translating pinhole profilers that typically require moving the mechanical pinhole at approximately 10,000 locations over the beam zone, a process that is especially susceptible to repeatability issues. In comparison, the proposed analyzer has an inherent 100% accurate digital pinhole location with the DMD chip structure, which leads to a powerful attribute for multimode laser beam characterization.

## 5. Conclusion

For the first time to our knowledge, a laser beam propagation analyzer system using a liquid ECVFL and a DMD has been proposed and demonstrated. Analyzer experiments conducted with a 633 nm wavelength laser beam of manufacturer-defined parameters show the analyzer to accurately measure the beam specifications. This analyzer can be used not only to precisely determine the parameters of a single-mode Gaussian laser beam as demonstrated but can also be used to measure multimode laser beam parameters. The proposed analyzer uses complete electronic control and eliminates the need for any motion of precision optics, thus promising excellent reliability, speed, and repeatability. Future research will focus on experimentally demonstrating the  $M^2$  measurement capability of the analyzer.

The authors thank Nuonics, Inc. for providing the equipment for the experiments.

## References

1. H. Kogelnik and T. Li, "Laser beams and resonators," *Appl. Opt.* **5**, 1550–1567 (1966).
2. J. E. Sollid, C. R. Phipps, Jr., S. J. Thomas, and E. J. McLellan, "Lensless method of measuring Gaussian laser beam divergence," *Appl. Opt.* **17**, 3527–3529 (1978).
3. J. A. Arnaud, W. M. Hubbard, G. D. Mandeville, B. de la Clavière, E. A. Franke, and J. M. Franke, "Technique for fast measurement of Gaussian laser beam parameters," *Appl. Opt.* **10**, 2775–2776 (1971).
4. Y. Suzuki and A. Tachibana, "Measurement of the Gaussian laser beam divergence," *Appl. Opt.* **16**, 1481–1482 (1977).
5. J. Falk, "Measurement of laser beam divergence," *Appl. Opt.* **22**, 1131–1132 (1983).
6. R. M. Herman, J. Pardo, and T. A. Wiggins, "Diffraction and focusing of Gaussian beams," *Appl. Opt.* **24**, 1346–1354 (1985).

7. S. Nemoto, "Determination of waist parameters of a Gaussian beam," *Appl. Opt.* **25**, 3859–3863 (1986).
8. T. F. Johnston, Jr., "Beam propagation ( $M^2$ ) measurement made as easy as it gets: the four-cuts method," *Appl. Opt.* **37**, 4840–4850 (1998).
9. W. Plass, R. Maestle, K. Wittig, A. Voss, and A. Giesen, "High-resolution knife-edge laser beam profiling," *Opt. Commun.* **134**, 21–24 (1997).
10. D. R. Skinner and R. E. Whitcher, "Measurement of the radius of a high-power laser beam near the focus of a lens," *J. Phys. E* **5**, 237–238 (1972).
11. P. J. Brannon, J. P. Anthes, G. L. Cano, and J. E. Powell, "Laser focal spot measurements," *J. Appl. Phys.* **46**, 3576–3579 (1975).
12. P. J. Shayler, "Laser beam distribution in the focal region," *Appl. Opt.* **17**, 2673–2674 (1978).
13. C. P. Wang, "Measuring 2-D laser-beam phase and intensity profiles: a new technique," *Appl. Opt.* **23**, 1399–1402 (1984).
14. H. Dittlacher, J. R. Krenn, A. Leitner, and F. R. Aussenegg, "Surface plasmon polariton-based optical beam profiler," *Opt. Lett.* **29**, 1408–1410 (2004).
15. M. K. Giles and E. M. Kim, "Linear systems approach to fiber characterization using beam profile measurements," *Proc. SPIE* **500**, 67–70 (1984).
16. S. Sumriddetchkajorn and N. A. Riza, "Micro-electromechanical system-based digitally controlled optical beam profiler," *Appl. Opt.* **41**, 3506–3510 (2002).
17. N. A. Riza, "Digital optical beam profiler," U.S. patent 6,922,233 (26 July 2005).
18. N. A. Riza and M. J. Mughal, "Optical power independent optical beam profiler," *Opt. Eng.* **43**, 793–797 (2004).
19. N. A. Riza and F. N. Ghauri, "Super resolution hybrid analog-digital optical beam profiler using digital micro-mirror device," *IEEE Photon. Technol. Lett.* **17**, 1492–1494 (2005).
20. M. Sheikh and N. A. Riza, "Demonstration of pinhole laser beam profiling using a digital micro-mirror device," *IEEE Photon. Technol. Lett.* **21**, 666–668 (2009).
21. M. Gentili and N. A. Riza, "Wide-aperture no-moving-parts optical beam profiler using liquid-crystal displays," *Appl. Opt.* **46**, 506–512 (2007).
22. M. W. Sasnett, "Propagation of multimode laser beams—the  $M^2$  factor," in *Physics and Technology of Laser Resonators*, D. R. Hall and P. E. Jackson, eds. (Hilger, 1989), Chap. 9, pp. 132–142.
23. A. E. Siegman, "How to (maybe) measure laser beam quality," in *Vol. 17 of OSA Trends in Optics and Photonics*, pp. 184–199 (Optical Society of America, 1998).
24. *Model Arctic 320 Liquid Lens Technical Data Sheet: Optical and Opto-Mechanical Data* (Varioptic, SA., Lyon, France, 2006), p. 1.
25. P. Ruffin, "Autofocus liquid lenses target new applications," *Opt. Laser Europe Mag.*, pp. 17–20 (October 2007).
26. K. Levenberg, "A method for the solution of certain non-linear problems in least squares," *Q. Appl. Math.* **2**, 164–168 (1944).
27. "Test methods for laser beam parameters: beam widths, divergence angle, and beam propagation factor," ISO/TC 172/SC9/WG1, ISO/DIS 11146, available from Deutsches Institut für Normung, Pforzheim, Germany.
28. M. W. Sasnett and T. F. Johnston, Jr., "Apparatus for measuring the mode quality of a laser beam," U.S. patent 5,214,485 (25 May 1993).
29. A. E. Siegman and S. W. Townsend, "Output beam propagation and beam quality from a multimode stable-cavity laser," *IEEE J. Quantum Electron.* **29**, 1212–1217 (1993).